J|A|C|S COMMUNICATIONS

Published on Web 09/01/2009

Metal−Organic Frameworks As Templates for Nanoscale $NaAlH_4$

Raghunandan K. Bhakta,[†] Julie L. Herberg,[‡] Benjamin Jacobs,[†] Aaron Highley,[†] Richard Behrens, Jr.,[†] Nathan W. Ockwig,[§] Jeffery A. Greathouse,[§] and Mark D. Allendorf*,[†]

Sandia National Laboratories, Livermore, California 94551-0969, Lawrence Livermore National Laboratories, Livermore, California 94550, and Sandia National Laboratories, Albuquerque, New Mexico 87185

Received June 5, 2009; E-mail: mdallen@sandia.gov

Metal hydrides are the focus of intensive research for vehicular hydrogen storage. Although some light-metal hydrides can meet the gravimetric and volumetric capacity requirements, their strong, directional chemical bonds lead to high thermodynamic stability, sluggish desorption kinetics, and limited reversibility.[1] Additives,[2] doping,[3] and alloying[4] to modify the desorption thermodynamics and catalysts[3] and accelerate kinetics so far yield limited improvements for many attractive light-metal hydrides.

Recent theoretical evidence suggests that reducing some binary metal hydrides (MgH_2[5] and NaH[5b]) to dimensions on the nanoscale decreases their H_2 desorption enthalpy. Experimental data are also encouraging, but disagree with theory. Aerogels, nanofibers, and ordered mesoporous silica infiltrated with MgH_2,[6a] $LiBH_4$,[6b] and $NaAlH_4$[6c] desorb H_2 at temperatures lower than bulk, but the wide range of particle sizes (2 nm to 10 μm) makes it impossible to validate theory and establish the onset of these effects. The chemical environment surrounding the particle may also play a role.[6a,7] A new synthetic platform is needed that provides control over both particle size and local chemical environment, so that the origin of nanoscale effects can be established. Unfortunately, the disorder inherent in many hard and soft templates makes it extremely difficult to synthesize uniform particles and understand their chemical environment.

Metal−organic frameworks (MOFs) offer an attractive alternative to these traditional scaffolds because their ordered crystalline lattice provides a highly controlled and inherently understandable environment. Moreover, MOFs have a degree of synthetic flexibility unmatched by other nanoscale templates, allowing pore shape, size, and chemistry to be systematically tailored. Fischer et al. were the first to show that MOFs could be used as templates for transition-metal nanoclusters.[8] We expand this concept by showing that MOFs are stable hosts for metal hydrides and their reactive precursors. Using $NaAlH_4$ as an example, we show that confining a hydride to the well-defined pores of the MOF HKUST-1 yields particles with greatly accelerated H_2 desorption kinetics compared to the bulk.

We selected HKUST-1 ($Cu_3(BTC)_2$) as a template for detailed investigation (BTC = benzene tricarboxylate) because its pore openings are much smaller than the interior dimensions, which should limit nanoparticle mobility (4 pores/unit cell with 9 Å × 9 Å openings and 11 Å × 16 Å interior dimensions).[9] HKUST-1 is also thermally stable up to 250 °C, enabling H_2 desorption from several metal hydrides without decomposition.[9a,b] Dehydrated HKUST-1 was infiltrated with a solution of $NaAlH_4$ in THF, allowing straightforward comparisons with previous work using carbon nanofibers (Supporting Information, Table ST1).[6c] Infiltrated material **1** was heated to 110 °C under vacuum to remove physisorbed solvent, yielding **2**, which has 4.0 wt % $NaAlH_4$ by elemental analysis. On average there are eight THF molecules and eight formula units of $NaAlH_4$ per large pore in **2**. Powder X-ray diffraction (PXRD) patterns of **1** and **2** show that the MOF is unaffected by this high local concentration of $NaAlH_4$. The particle size cannot be determined by TEM because both $NaAlH_4$ and HKUST-1 are unstable in the electron beam.[10] The focused TEM beams required to image very small particles destroy the HKUST-1 crystal structure within a few seconds, causing the hydride nanoparticles to coalesce into large, multielement particles (5−10 nm; Figure S13a,c) that are not representative of the infiltrated material.

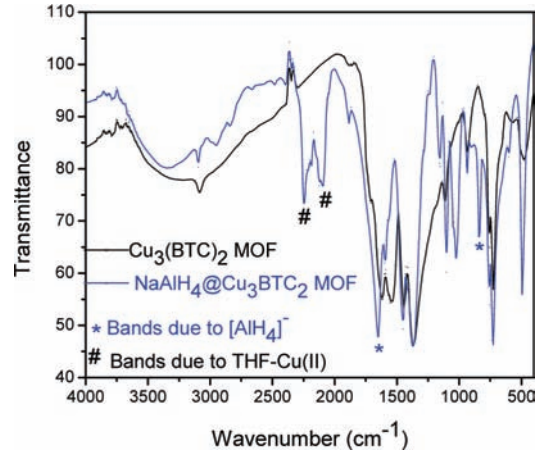

Figure 1. IR spectrum of neat $Cu_3(BTC)_2$ MOF (black) and $NaAlH_4$@ $Cu_3(BTC)_2$ MOF (**2**, blue).

FTIR, PXRD, TEM/electron energy loss spectroscopy (EELS), microporosimetry, and magic-angle spinning NMR (MAS NMR) provide strong evidence that infiltrated $NaAlH_4$ exists as clusters within the MOF pores. PXRD of **2** exhibits no specific reflections corresponding to $NaAlH_4$, indicating that the clusters are either amorphous or too small to be observed. The FTIR spectrum of **2** (Figure 1), however, exhibits intense bands at 1653 and 845 cm^{-1}, corresponding to the ν_3 $[AlH_4]^-$ stretching and ν_4 $[AlH_4]^-$ bending modes.[11] New bands in the 2090−2249 cm^{-1} region are assigned to THF coordinated to axial sites in the $Cu_2(CO_2)_4$ paddlewheel units, as are resonances at −4.63 ppm and −7.88 ppm in the ^{1}H MAS NMR (Figure S3). These disappear upon prolonged heating under high vacuum. A TEM/EELS map with 1-nm spatial resolution shows Al is uniformly distributed throughout the crystals of **2** (Figure S13b), and the BET surface area of **2** (762 m^2 g^{-1}) is much lower than activated HKUST-1.[9a] Finally, MAS NMR data (Figure S5−S7) suggest that, in the presence of physisorbed THF in **1**, the hydride exists as a dissociated ion pair, similar to $LiAlH_4$ in THF.[12b] Upon removal of this guest solvent to form **2**, the ions reassociate. The ^{23}Na MAS NMR of **1** exhibits a resonance at −1.8 ppm, while in **2** this signal is shifted upfield to

[†] Sandia National Laboratories, Livermore, California.
[‡] Lawrence Livermore National Laboratories.
[§] Sandia National Laboratories, Albuquerque, New Mexico.

10.1021/ja904431x CCC: $40.75

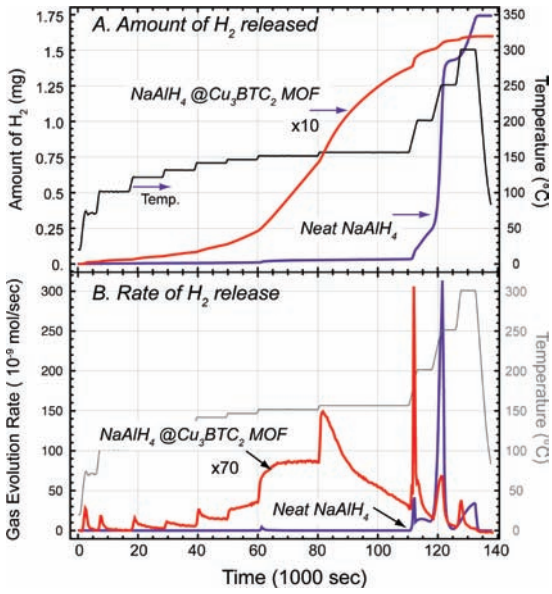

Figure 2. (A) Amount of H_2 released from **2** compared with neat $NaAlH_4$ and (B) rate of H_2 released from $NaAlH_4$@MOF compared with neat $NaAlH_4$. Stepped line in each plot indicates the temperature profile. H_2 desorbed from neat $NaAlH_4$ at ~180 °C is due to incongruent melting and at ~300 °C is due to NaH, coincident with detection of Na vapor.

−9.4 ppm, similar to neat $NaAlH_4$.[12] Similarly, a peak at 96.2 ppm is evident in the ^{27}Al MAS NMR of **1**, while in **2** the signal is shifted slightly upfield to 94.4 ppm. Neat $NaAlH_4$ has a chemical shift of 94.6 ppm.[12] The ^{27}Al and ^{23}Na resonances in **2** are broadened relative to **1**, indicating reduced mobility for both ions. ^{1}H MAS NMR signals associated with $NaAlH_4$ protons have a longer relaxation time relative to the linker protons and are only visible with a relaxation time 20 s at 3.09 ppm (Figure S4). In aggregate these data support the conclusion that the $NaAlH_4$ exists as small (≤1.5 nm), possibly amorphous clusters, within the MOF pores. An alternative explanation, that the $NaAlH_4$ is supported on the outside of the MOF crystals, disagrees with both EELS and PXRD data. Such a layer would be >6 nm thick (based on an estimated 1 μm average crystallite size) and very likely crystalline after the prolonged heating cycle to remove solvent.

The H_2 desorption behavior of **2** is very different from bulk $NaAlH_4$. Although a detailed understanding of the mechanism is beyond the scope of this paper, our initial results (obtained from simultaneous thermogravimetric modulated-beam mass spectrometry,[13a,b] a technique we developed to characterize reaction networks of complex processes[13c]) show that multiple chemical and/or physical processes are involved. We used deuterated THF to eliminate interference with the $m/z = 2$, H_2 signal from $NaAlH_4$ and temperature profiles (e.g., Figure 2) consisting of a series of isothermal steps to expose individual reaction processes. Neat $NaAlH_4$ desorbs 70% of its H_2 at $T \approx 250$ °C (Figure 2A), consistent with the literature.[3] In contrast, $NaAlH_4$ confined within the MOF pores desorbs H_2 at much lower temperatures. H_2 is initially observed at 70 °C, followed by a series of desorption events at higher temperatures (Figure 2B). The first five isothermal steps are characterized by an initial rapid H_2 release that then decays to a steady-state value. At the 145 and 150 °C isothermal steps, the rate increases with time. These combined behaviors are consistent with a nucleation step at low T and growth at high T.[13c] The H_2 desorption rate peaks at 155 °C and then decays as the hydrogen is depleted. At this stage, ~80% of the total H_2 is desorbed from the sample (Figure 2A). The nanoscale hydride thus decomposes at ~100 °C lower than bulk $NaAlH_4$. PXRD of **2** heated to 160 °C (**3**; Figure S12) shows the MOF is not decomposed by $NaAlH_4$ decomposition. The data also indicate that during the early isothermal steps of the experiment (up to ~30000 s), H_2 and THF(D) evolution are correlated (Figure S2). This suggests that nanoscale effects result from a combination of reduced size and the local chemical environment confining the clusters.

We conclude that MOFs are effective templates for the formation of nanoscale $NaAlH_4$. In addition to HKUST-1, we find that other MOFs (e.g., MIL-68[14] and MOF-5[14b]) can be infiltrated with hydrides or hydride precursors (e.g., $Mg(C_4H_9)_2$ and LiC_2H_5) without degradation. MOF-5 may be less useful because H_2O within the pores desorbs as high as 300 °C and may react with the hydride. The $NaAlH_4$ described here is of a size consistent with the onset of nanoscale effects predicted for simple hydrides,[5] although the role of the pore chemistry also must be established. We are now extending the methods developed here to other metal hydrides and MOFs with a variety of pore dimensions, metal centers, and linkers. By systematically varying such parameters it should be possible to identify the factors controlling nanoscale hydride stability, creating the potential for hydrogen storage materials with vastly improved desorption kinetics.

Acknowledgment. This work was funded by the US DOE Hydrogen, Fuel Cells, and Infrastructure Technologies Program. Work by J.L.H. was performed under the auspices of the U.S. DOE by Lawrence Livermore National Laboratory under Contract DE-AC52-07NA27344. The authors thank Miles Clift for XRD and Prof. Eric Majzoub for helpful discussions.

Supporting Information Available: Synthetic methods, NMR, EELS, EDX, XRD, desorption data, and TEM micrographs. This material is available free of charge via the Internet at http://pubs.acs.org.

References

(1) Grochala, W.; Edwards, P. P. *Chem. Rev.* **2004**, *104*, 1283.
(2) Alapati, S. V.; Johnson, J. K.; Sholl, D. S. *J. Phys. Chem. B* **2006**, *110*, 8769.
(3) Bogdanović, B.; Schwickardi, M. *J. Alloys Compd.* **1997**, *1*, 253.
(4) Zaluska, A.; Zaluski, L.; Strom-Olsen, J. O. *Appl. Phys. A* **2001**, *72*, 157. (b) Higuchi, K.; Kajioka, H.; Toiyama, K.; Fujii, H.; Orimo, S.; Kikuchi, Y. *J. Alloys Compd.* **1999**, *295*, 484. (c) Orimo, S.; Fujii, H. *Appl. Phys. A* **2001**, *72*, 167.
(5) Wagemans, R. W. P.; van Lenthe, J. H.; de Jongh, P. E.; Jos van Dillen, A.; Jong, K. P. d. *J. Am. Chem. Soc.* **2005**, *127*, 16675. (b) Kim, K. C.; Dai, B.; Johnson, J. K.; Sholl, D. S. *Nanotechnology* **2009**, *20*, 204001.
(6) (a) Kondo-Francois, A.-Z.; Ares-Fernández, J.-R. *Chem. Mater.* **2007**, *20*, 376. (b) Zhang, Y.; Zhang, W.-S.; Wang, A.-Q.; Sun, L.-X.; Fan, M.-Q.; Chu, H.-L.; Sun, J.-C.; Zhang, T. *Int. J. Hydrogen Energy* **2007**, *32*, 3976. (c) Baldé, C. P.; Hereijgers, B. P. C.; Bitter, J. H.; Jong, K. P. d. *J. Am. Chem. Soc.* **2008**, *130*, 6761. (d) Vajo, J. J.; Skeith, S. L.; Mertens, F. *J. Phys. Chem. B* **2005**, *109*, 3719.
(7) Berseth, P. A.; Harter, A. G.; Zidan, R.; Blomqvist, A.; Moyseś, C.; Araú, jo.; Scheicher, R. H.; Ahuja, R.; Jena, P. *Nano Lett.* **2009**, *9*, 1501–1505.
(8) Schröder, F.; Esken, D.; Cokoja, M.; van den Berg, M. W. E.; Lebedev, O. I.; Van Tendeloo, G.; Walaszek, B.; Buntkowsky, G.; Limbach, H.-H.; Chaudret, B.; Fischer, R. A. *J. Am. Chem. Soc.* **2008**, *130*, 6119.
(9) (a) Chui, S. S.-Y.; Samuel, M.-F. Lo.; Jonathan, P. H. Charmant; Orpen, A. G.; Williams, I. D. *Science* **1999**, *283*, 1148. (b) Schlichte, K.; Kratzke, T.; Kaskel, S. *Microporous Mesoporous Mater.* **2004**, *73*, 81.
(10) (a) Felderhoff, M.; Klementiev, K.; Grunert, W.; Spliethoff, B.; Tesche, B.; von Colbe, J. M.; Bogdanovic, B.; Hartel, M.; Pommerin, A.; Schuth, F.; Weidenthaler, C. *Phys. Chem. Chem. Phys.* **2004**, *6*, 4369. (b) Bogdanovic, B.; Brand, R. A.; Marjanovic, A.; Schwickardi, M.; Tolle, J. *J. Alloys Compd.* **2000**, *302*, 36.
(11) Gomes, S.; Renaudin, G.; Hagemann, H.; Yvon, K.; Sulic, M. P.; Jensen, C. M. *J. Alloys Compd.* **2005**, *390*, 305.
(12) Majzoub, E. H.; Herberg, J. L.; Stumpf, R.; Spangler, S.; Maxwell, R. S. *J. Alloys Compd.* **2005**, *394*, 265. (b) Bikiel, D. E.; Salvo, F. D.; Lebrero, M. C. G.; Doctorovich, F.; Estrin, D. A. *Inorg. Chem.* **2005**, *44*, 5286.
(13) (a) Behrens, R. *Rev. Sci. Instrum.* **1987**, *58*, 451. (b) Behrens, R. *Int. J. Chem. Kinet.* **1990**, *22*, 159–157. (c) Behrens, R. In *Overviews of Recent Research on Energetic Materials*; Shaw, R. W., Brill, T. B., Thompson, D. L., Eds., World Scientific Publishing Co.: Singapore, 2005; p 29.
(14) Volkringer, C.; Meddouri, M.; Loiseau, T.; Guillou, N.; Marrot, J.; Ferey, G.; Haouas, M.; Taulelle, F.; Audebrand, N.; Latroche, M. *Inorg. Chem.* **2008**, *47*, 11892. (b) Mohamed, E.; Hailian, Li.; Yaghi, O. M. *J. Am. Chem. Soc.* **2000**, *122*, 1391.

JA904431X